Self-Consistent Field Theory of Ordered Block Copolymer Blends. 1. $(AB)_\alpha/(AB)_\beta$ Blends

Richard J. Spontak

Department of Materials Science & Engineering, North Carolina State University, Raleigh, North Carolina 27695-7907

Received April 6, 1994; Revised Manuscript Received June 30, 1994[•]

ABSTRACT: Numerous theoretical efforts have been developed to identify molecular–morphological relationships in ordered AB diblock copolymers, but relatively few studies have sought to elucidate similar relationships in blends composed of two strongly segregated diblock copolymers, $(AB)_\alpha$ and $(AB)_\beta$. Since block mixing occurs at the molecular level in miscible $(AB)_\alpha/(AB)_\beta$ blends, relatively precise control over morphological development and microstructural dimensions can be achieved without the need to synthesize tailored materials. With the junctions of the α and β copolymer molecules confined to interphase regions at equilibrium in the strong-segregation regime, $(AB)_\alpha/(AB)_\beta$ blends may be envisioned as a bidisperse mixture of grafted chains and prove more well-behaved than copolymer/homopolymer blends. In this work, a self-consistent field theory is proposed for binary diblock copolymer blends possessing the lamellar morphology. Analytical expressions and corresponding predictions for the free energy and microdomain periodicity are provided for blends in which the constituent copolymers differ in composition and chain length. Predicted blend periodicities are in quantitative agreement with recent experimental results.

Introduction

Experimental efforts designed to elucidate the phase behavior of strongly segregated AB diblock copolymers have traditionally relied upon custom-synthesized materials to identify key molecular–morphological relationships. Recent developments[1–4] in anionic polymerization have greatly facilitated production of specialty diblock copolymers, but commercial use of neat copolymers to control morphology for novel applications ranging from monoporous ultrafilters[5] to biomimetic templates[6] may not be economically viable. A more promising route to tailor block copolymer morphologies is through molecular blending, in which mixing of the constituent species occurs within ordered microdomains. Miscible copolymer blends can provide fundamental insight into intramicrodomain mixing and chain packing, as well as commercial access to morphologies possessing relatively narrow composition ranges, such as the ordered bicontinuous double-diamond (OBDD)[7] and gyroid[8] morphologies.

Studies of miscible copolymer/homopolymer (AB/hA) blends, each consisting of a poly(styrene-*b*-isoprene) (SI) diblock copolymer and a parent homopolystyrene (hS), have demonstrated that intermediate (e.g., OBDD, cylindrical, or spherical) morphologies[9,10] and morphologies with controlled dimensions[11–13] can be generated with a lamellar copolymer through judicious choice of added hS. Factors governing ultimate morphological development, as well as the magnitude of repulsive monomer interactions,[14] have been found to include the blend composition and the hS chain length relative to the S block length, in quantitative agreement with predictions from recent theoretical treatments.[15,16] In this same vein, intermediate morphologies have also been observed in studies of AB/hC blends (hC refers to a nonparent homopolymer) composed of an ordered SI copolymer and either poly(propylene oxide)[17,18] or poly(vinyl methyl ether).[19]

Another route to controlling copolymer morphology is through the use of miscible diblock copolymer/copolymer, $(AB)_\alpha/(AB)_\beta$, blends. Unlike AB/hA blends consisting of confined, yet mobile,[20] homopolymer molecules, both constituent species in $(AB)_\alpha/(AB)_\beta$ blends are conformationally constrained due to the restriction that, at equilibrium, all block junctions must reside within the interphase regions separating adjacent microdomains. As illustrated in Figure 1, relatively short blocks can be envisioned as grafted blobs lying in close proximity to the interphase. Long blocks, on the other hand, presumably adopt a mushroom shape to satisfy volume-filling requirements. Hashimoto et al.[21,22] and Hadziioannou and Skoulios[23] have shown that the microdomain periodicity (D in Figure 1) can be finely adjusted in $(AB)_\alpha/(AB)_\beta$ blends exhibiting the lamellar morphology, whereas Schwark[24] and Spontak et al.[25] have found that intermediate morphologies can be produced in binary blends of lamellar and nonlamellar copolymers.

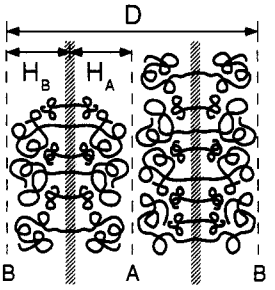

Figure 1. Illustration of the lamellar morphology generated in a miscible blend of strongly segregated diblock copolymers. Since the blocks of the α and β copolymers in this $(AB)_\alpha/(AB)_\beta$ blend mix at the molecular level within their respective microdomains, morphological characteristics can be tailored through judicious choice of constituent copolymers and blend composition. Microstructural dimensions, such as the lamellar half-width (H_i, i = A or B) and periodicity (D), are also displayed here.

While these experimental results indicate that morphologies can be controlled through the use of miscible $(AB)_\alpha/(AB)_\beta$ blends, few theoretical treatments have been developed to address the ordered microstructure[26–28] or conformational characteristics[29,30] of such blends. In this work, a self-consistent field (SCF) theory based on the pioneering efforts of Semenov[31] and Zhulina and Halperin[32] (for neat diblock and triblock copolymers, respectively) is proposed for binary $(AB)_\alpha/(AB)_\beta$ blends of lamellar diblock copolymers.

[•] Abstract published in *Advance ACS Abstracts,* September 15, 1994.

0024-9297/94/2227-6363$04.50/0

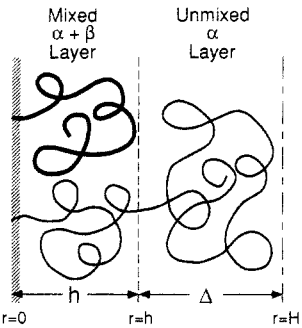

Figure 2. Schematic diagram of a single lamella (either A or B) occupied by both α and β copolymer molecules. If r denotes the coordinate axis along the lamellar normal, then all of the β monomers, N_β, reside with a fraction of α monomers, ΓN_α, in the layer between $r = 0$ and $r = h$. The remainder of α monomers, $(1 - \Gamma)N_\alpha$, is deposited in the Δ layer between $r = h$ and $r = H$. Both copolymer species are nonuniformly stretched.

Theoretical Formalism

As depicted in Figure 1, two strongly segregated AB diblock copolymers, α and β, differing in composition and chain length are envisioned to microphase-separate into a single lamellar morphology. The free energy of each copolymer, relative to a melt of identical, but disconnected, blocks must take into account the (i) elastic deformation of the blocks confined in microdomain space and (ii) repulsive monomer interactions localized at the interphase. These contributions, on a per area basis, are denoted as F_i (i = A or B) and F_{AB}, respectively. Since the A and B blocks of both copolymers are mixed within their respective microdomains, the free energy (F) must also include terms representing intramicrodomain mixing ($F_{i,mix}$) so that

$$F = F_{AB} + F_A + F_B + F_{A,mix} + F_{B,mix} \quad (1)$$

In the strong-segregation regime wherein repulsive A–B interactions dominate and $\chi_{AB} N \gg 10$ (χ_{AB} is the Flory–Huggins interaction parameter between A and B monomers and N constitutes the total number of monomers), the narrow interphase approximation of Helfand and Wasserman[33] is valid and therefore implemented, in which case F_{AB} is independent of chain length. If the α and β copolymers are both ordered, it immediately follows that F_{AB} is also independent of blend composition. Since two interphases exist within D (see Figure 1) and if the monomer volume (b^3, where b denotes monomer length) is set equal to unity, F_{AB} can be written as

$$\frac{F_{AB}}{kT} = \frac{2b}{6^{1/2}} \chi_{AB}^{1/2} \quad (2)$$

where k is the Boltzmann constant and T denotes absolute temperature.

Unlike F_{AB}, the elastic energy contributions to F are sensitive to block conformations and packing. The SCF approach taken by Zhulina and Halperin[32] explicitly addresses the bridged and looped midblock conformations of lamellar triblock copolymers and is therefore adopted here. A lamella is presumed to be symmetric about its midplane ($r = H$), in which case only one-half of a lamella, as illustrated in Figure 2, need be considered further. In this region, nonuniformly stretched blocks of two different lengths (N_α and N_β) are confined. Since, by arbitrary choice, the β block is shorter than the α block and is incapable of stretching to H, a boundary layer must exist in which all of the β blocks reside alongside a fraction of the α blocks. The fraction of α monomers occupying this mixed layer, which extends from the interphase at $r = 0$ to $r = h$, is denoted Γ. Likewise, a central core containing $N_\alpha(1-\Gamma)$ α monomers only extends from h to H over a distance Δ. The elastic free energy of each lamella is therefore the sum of the elastic free energies obtained from these two discrete layers:

$$F_i = 2F_{i,h} + 2F_{i,\Delta}, \quad i = A \text{ or } B \quad (3)$$

To facilitate derivation of $F_{i,h}$ and $F_{i,\Delta}$, the mixed (h) and unmixed (Δ) layers will be considered separately in the following sections. The functional forms of the elastic free-energy expressions are identical for the A and B blocks, and the subscript i will be omitted until these contributions are combined to obtain the final expression for F (eq 1).

I. Mixed (h) Layer. The total number of monomers occupying this region is $n_\alpha \Gamma N_\alpha + n_\beta N_\beta$, where n_i (i = α or β) denotes the number of moles of component i present, and an average monomer number ($\bar{N}$) for this layer can be expressed as $x_\alpha \Gamma N_\alpha + (1 - x_\alpha)N_\beta$, where x_α (hereafter referred to as x) is the mole fraction of α. For convenience, ϵ is defined as N_β/N_α so that $\bar{N} = \xi N_\alpha$, where $\xi \equiv x\Gamma + \epsilon(1 - x)$. The ratio Γ/ϵ relates the number of α monomers within the layer to the total of β monomers.

The elastic free energy is sensitive to the number of fixed block ends. Short β chains, for instance, are restricted at only one end (at $r = 0$). In the nomenclature of Zhulina and Halperin,[32] the free end (η) of each β block lies between $r = 0$ and $r = h$, and the probability distribution of finding η within the spatial interval $d\eta$ is $g(\eta)\, d\eta$. In contrast, the longer α blocks extend beyond $r = h$ into the unmixed core. Thus, the nonuniformly stretched α blocks occupying the mixed layer can be considered restricted at both $r = 0$ and $r = h$. If $E_j(r,y)$ denotes the local free energy of elastic deformation of block j along the lamellar normal and y corresponds to the position of the end of block j, the elastic free energy of the mixed layer can be expressed as

$$\frac{F_h'}{kT} = \frac{3}{2b^2}[x \int_0^h E_\alpha(r,h)\, dr + (1 - x) \int_0^h g(\eta)\, d\eta \int_0^\eta E_\beta(r,\eta)\, dr] \quad (4)$$

where the prime on F_h signifies a per chain basis. Since h is independent of r, $E_\alpha(r,h)$ will hereafter be abbreviated $E_\alpha(r)$. Equation 4 is subject to boundary conditions which (i) conserve the number of monomers of each chain within the mixed layer and (ii) guarantee that the polymer density within the layer is uniform. The conditions reflecting conservation of mass are

$$\int_0^\eta E_\beta^{-1}(r,\eta)\, dr = \epsilon N_\alpha \quad (5a)$$

$$\int_0^h E_\alpha^{-1}(r)\, dr = \Gamma N_\alpha \quad (5b)$$

In the melt, the local polymer volume fraction, $\Phi_h(r)$, must equal unity, in which case

$$\Phi_h(r) = \frac{b^3}{\sigma}[xE_\alpha^{-1}(r) + (1 - x) \int_r^h g(\eta) E_\beta^{-1}(r,\eta)\, d\eta] = 1 \quad (6)$$

where σ is the monomer surface area. Minimization of eq 4 subject to eqs 5 and 6 is achieved through the use of Lagrange multipliers and results in

$$E_\beta(r,\eta) = (\pi/2\epsilon N_\alpha)(\eta^2 - r^2)^{1/2} \quad (7a)$$

$$E_\alpha(r) = (\pi/2\epsilon N_\alpha)(\Lambda^2 - r^2)^{1/2} \quad (7b)$$

where $\Lambda = h \csc(\pi\Gamma/2\epsilon)$. Incorporation of eq 7 into eq 4 can be shown to yield

$$\frac{F_h'}{kT} = \frac{\pi^2\sigma h^3}{8b^5(\epsilon N_\alpha)^2} + \frac{3\pi x h^2}{4b^2\epsilon N_\alpha}\cot\left(\frac{\pi\Gamma}{2\epsilon}\right) \quad (8)$$

The derivation of eqs 7 and 8 is provided in the Appendix.

Except for nomenclature differences, eq 8 is identical to earlier results obtained[32] for a similar boundary layer containing looped and bridged midblocks in lamellar triblock copolymers. Incompressibility of the melt dictates[34] that $h\sigma = b^3 N_\alpha \xi$ and $H\sigma = b^3 N_\alpha \mu$, where $\mu = x + \epsilon(1 - x)$. Substituting these relationships into eq 8 and dividing by σ results in F_h:

$$\frac{F_h}{kT} = \frac{\pi^2 H^3 \xi^3}{8b^2(\epsilon N_\alpha)^2\mu^3}\left[1 + \frac{6\epsilon x}{\pi\xi}\cot\left(\frac{\pi\Gamma}{2\epsilon}\right)\right] \quad (9)$$

In the limit of pure β copolymer, $x = 0$, $\xi = \mu$, and eq 9 reduces to

$$\frac{F_h}{kT} = \frac{\pi^2 H^3}{8b^2 N_\beta^2} \quad (10)$$

This expression is analogous to the one derived by Semenov[31] for neat diblock copolymers if the monomer gyration radius ($a = b/6^{1/2}$) is used rather than b and a factor of 2 is introduced to account for the two half-lamellar A or B regions per D.

Mixing of the α and β blocks occurs only within the layer bounded by $r = 0$ and $r = h$. The corresponding free energy of random mixing can be expressed as

$$\frac{F_{mix}'}{kT} = \Sigma(x) \quad (11)$$

where $\Sigma(x) \equiv x \ln x + (1 - x)\ln(1 - x)$. As in the case of F_h', F_{mix}' can be rewritten on a per area basis by recalling the incompressibility constraints governing h and H. Thus

$$\frac{F_{mix}}{kT} = \frac{H\Sigma(x)}{N_\alpha\mu} \quad (12)$$

II. Unmixed (Δ) Layer. Unlike the mixed $\alpha + \beta$ layer, the central core consists only of monomers deposited from the α block. Each α segment is anchored at one end ($r = h$) and unrestricted at the other, resulting in nonuniformly stretched segments. Note that nonuniform stretching of the block segments occupying Δ distinguishes ordered $(AB)_\alpha/(AB)_\beta$ diblock copolymer blends from ABA triblock copolymers wherein uniformly stretched bridged B blocks comprise the unmixed central layer. The elastic free energy of the α segment in Δ can be written in an analogous fashion as eq 4, namely,

$$\frac{F_\Delta'}{kT} = \frac{3x}{2b^2}\int_h^H g(\delta)\,d\delta \int_h^\delta E_\alpha(r,\delta)\,dr \quad (13)$$

where δ denotes the position of the free end. As in the case of F_h', F_Δ' must satisfy the following conservation requirements:

$$\int_h^\delta E_\alpha^{-1}(r,\delta)\,dr = N_\alpha(1 - \Gamma) \quad (14)$$

and

$$\Phi_\Delta(r) = \frac{xb^3}{\sigma}\int_r^H g(\delta)E_\alpha^{-1}(r,\delta)\,d\delta = 1 \quad (15)$$

Minimization of eq 13 subject to eqs 14 and 15 leads to

$$E_\alpha(r,\delta) = \pi[2(1 - \Gamma)N_\alpha]^{-1}(\delta^2 - r^2)^{1/2} \quad (16)$$

which, upon substitution into eq 13 and incorporation of the incompressibility criterion $h/H = \xi/\mu$, yields

$$\frac{F_\Delta'}{kT} = \frac{\pi^2\sigma H^3 x}{16b^5(1 - \Gamma)^2 N_\alpha^2}[2 - 3\xi/\mu + (\xi/\mu)^3] \quad (17)$$

The bracketed factor in eq 17 can be simplified by recognizing that $\xi = \mu - x(1 - \Gamma)$. Thus, the elastic free energy of the unmixed layer per area is given by

$$\frac{F_\Delta}{kT} = \frac{\pi^2 H^3 x^3}{16b^2 N_\alpha^2\mu^2}[3 - x(1 - \Gamma)/\mu] \quad (18)$$

In the limit that the blend consists of pure α copolymer, $x = 1$, $\mu = 1$, and $\Gamma = 0$ (since the mixed layer would not exist). Equation 18 correctly reduces to eq 10, with N_β replaced by N_α. If, on the other hand, the blend is composed of only β copolymer, $x = 0$, $\mu = \epsilon$, and F_Δ collapses to zero.

III. Equilibrium Characteristics. According to Figure 1, a single microdomain period (D) is comprised of one A lamella and one B lamella, in which case the expressions derived for F_h, F_Δ, and F_{mix} must be multiplied by a factor of 2. In addition, the monomer length b is assumed to be the same for the A and B monomers. Upon substitution of eqs 9, 12, and 18 into eq 1, the free energy (F) corresponding to the length scale D can be written as

$$\frac{F}{kT} = \frac{\pi^2\Psi}{4b^2}\left(\frac{H_A^3}{N_{A,\alpha}^2} + \frac{H_B^3}{N_{B,\alpha}^2}\right) + \frac{2b}{6^{1/2}}\chi_{AB}^{1/2} + \frac{2\Sigma(x)}{\mu}\left(\frac{H_A}{N_{A,\alpha}} + \frac{H_B}{N_{B,\alpha}}\right) \quad (19)$$

where $N_{i,\alpha}$ (i = A or B) corresponds to the number of i monomers in the α copolymer and

$$\Psi \equiv \frac{\xi^2}{\epsilon^2\mu^3}\left[\xi + \frac{6\epsilon x}{\pi}\cot\left(\frac{\pi\Gamma}{2\epsilon}\right)\right] + \frac{x^3}{2\mu^3}[3\mu - x(1 - \Gamma)] \quad (19a)$$

Following Semenov,[31] the A and B blocks of the α copolymers can be related through f, the fraction of A monomers, equal to $N_{A,\alpha}/(N_{A,\alpha} + N_{B,\alpha})$. It immediately follows that $N_{B,\alpha} = N_{A,\alpha}(1/f - 1)$ and, since the melt is incompressible, $H_B = H_A(1/f - 1)$. The β copolymer is assumed here to possess the same f as the α copolymer. If these relationships are substituted into eq 19, F/kT simplifies to

$$\frac{F}{kT} = \frac{\pi^2 H_A^3\Psi}{4b^2 N_{A,\alpha}^2 f} + \frac{2b}{6^{1/2}}\chi_{AB}^{1/2} + \frac{4H_A\Sigma(x)}{\mu N_{A,\alpha}} \quad (20)$$

From Figure 1, D can be expressed as $2H_A + 2H_B$ or, equivalently, $2H_A/f$. Division of F by D therefore yields the free energy per volume ($\mathcal{F}$), viz.,

$$\frac{\mathcal{F}}{kT} = \frac{\pi^2 H_A^2\Psi}{8b^2 N_\alpha^2 f^2} + \frac{bf}{6^{1/2}H_A}\chi_{AB}^{1/2} + \frac{2\Sigma(x)}{\mu N_\alpha} \quad (21)$$

Minimization of $\mathcal{F}$ in eq 21 with respect to H_A and Γ

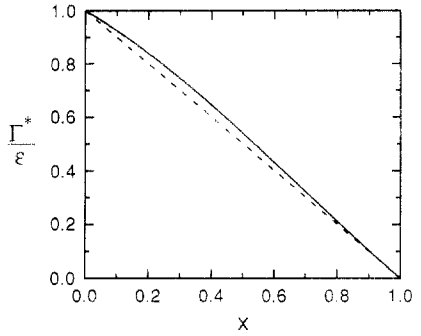

Figure 3. Dependence of Γ^*/ϵ on blend composition (x) at equilibrium. The solid line corresponds to eq 24, which is the result of minimizing $\mathcal{F}$ in eq 21 with respect to Γ, and is generally applicable to lamellar diblock copolymer blends. An empirical correlation describing this curve is provided in the text. Note that this curve does not differ significantly from the linear relationship $\Gamma^*/\epsilon = 1 - x$ (dashed line).

leads to the equilibrium microdomain periodicity ($D_{\alpha\beta}$) and the fraction of α monomers in h (Γ^*), respectively. Note that the mixing term is independent of both H_A and Γ and does not contribute to either $D_{\alpha\beta}$ or Γ^*. Evaluation of $(\partial\mathcal{F}/\partial H_A)_\Gamma = 0$, followed by algebraic rearrangement and substitution of D for H_A, results in

$$D_{\alpha\beta} = \frac{4}{6^{1/2}}\left(\frac{3}{\pi^2}\right)^{1/3} b N_\alpha^{2/3} \chi_{AB}^{1/6} \Psi^{-1/3} \tag{22}$$

Equation 22 is reminiscent of the result obtained by Semenov[31] for neat diblock copolymers, indicating that $D_{\alpha\beta}$, like D_α, scales as $N_\alpha^{2/3}$. In fact, $D_{\alpha\beta}/D_\alpha$ can be conveniently written as

$$\frac{D_{\alpha\beta}}{D_\alpha} = \Psi^{-1/3} \tag{23}$$

In the limit when $x = 1$, $\Psi = 1$ and $D_{\alpha,\beta} = D_\alpha$. Likewise, when $x = 0$, $\Psi = 1/\epsilon^2$ and, recalling that $(N_\alpha\epsilon)^{2/3} = N_\beta^{2/3}$, $D_{\alpha\beta} = D_\beta$.

Differentiation of $\mathcal{F}$ in eq 21 with respect to Γ at constant H_A yields the following expression for Γ^* at equilibrium:

$$\frac{\Gamma^*}{\epsilon} = 1 + \frac{2}{\pi}\tan\left(\frac{\pi\Gamma^*}{2\epsilon}\right)\left[1 + \left(1 + \frac{\pi^2 x}{24}\right)^{1/2}\right] - \frac{1}{x} \tag{24}$$

It is of interest to note that, according to eq 24, the ratio of α and β monomers residing in h (Γ^*/ϵ) depends only on blend composition (x). Once these relationships for $D_{\alpha\beta}$ and Γ^* are incorporated into eq 21, the minimized free energy function ($\mathcal{F}_{\alpha\beta}^*/kT$) for the α/β blend becomes

$$\frac{\mathcal{F}_{ab}^*}{kT} = \frac{1}{4}\left(\frac{9\pi^2\chi_{AB}\Psi}{N_\alpha^2}\right)^{1/3} + \frac{2\Sigma(x)}{\mu N_\alpha} \tag{25}$$

Since the first term is proportional to the minimum free energy of the pure α copolymer ($\mathcal{F}_\alpha^*$), eq 25 can be rewritten as

$$\frac{\mathcal{F}_{\alpha\beta}^*}{kT} = \frac{\mathcal{F}_\alpha^*}{kT}\Psi^{1/3} + \frac{2\Sigma(x)}{\mu N_\alpha} \tag{25a}$$

Results and Discussion

Values of Γ^*/ϵ determined by numerical methods from eq 24 are provided as a function of mole fraction in Figure 3. Irrespective of the block lengths of the α and β copolymers, a single $\Gamma^*/\epsilon(x)$ curve is predicted and is found to lie near the linear relationship $\Gamma^*/\epsilon = 1 - x$ (also shown for comparison in Figure 3). These results indicate that

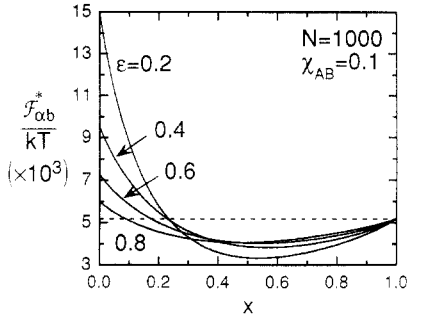

Figure 4. Variation of the minimum blend free energy ($\mathcal{F}_{\alpha\beta}^*/kT$) with blend composition for four values of ϵ: 0.2, 0.4, 0.6, and 0.8. Values of $\mathcal{F}_{\alpha\beta}^*$ at $x = 0$ and $x = 1$ correspond to $\mathcal{F}_\beta^*$ and $\mathcal{F}_\alpha^*$, respectively. In all four cases, the curves exhibit a minimum at an intermediate blend composition. The magnitude of the minimum is seen here to be relatively independent of ϵ over the range $0.4 \le \epsilon \le 0.8$. The dashed line corresponds to $\mathcal{F}_\alpha^*$.

the ratio Γ^*/ϵ can be approximated by $1-x$, but is more accurately described by

$$\frac{\Gamma^*}{\epsilon} = (1 - x)\,\phi \tag{26}$$

where $\phi = 1 + 0.3056x - 0.2968x^2$.

Equation 26 is used to obtain values of the minimum free energy ($\mathcal{F}_{\alpha\beta}^*/kT$ in eq 25) for four symmetric copolymer blends possessing $\chi_{AB} = 0.1$, $N_\alpha = 1000$, and ϵ ranging from 0.2 to 0.8. This choice of parameters satisfies not only the general strong-segregation requirement for each copolymer (i.e., $\chi_{AB}N_i > 10.5$, where i = α or β) but also the strong-segregation criterion proposed by Melenkevitz and Muthukumar[35] for the α copolymer (i.e., $\chi_{AB}N_\alpha \ge 100$). Results from eq 25 are displayed as a function of x in Figure 4 and reveal that each $\mathcal{F}_{\alpha\beta}^*/kT(x)$ curve initially decreases from $\mathcal{F}_\beta^*/kT$ (at $x = 0$), reaches a minimum, and then increases to $\mathcal{F}_\alpha^*/kT$ (at $x = 1$). The minimum is dependent on ϵ and, for $\epsilon < 1$, consistently lies below the equilibrium free energy of either constituent copolymer. Figure 4 also demonstrates that the shapes and minima of the $\mathcal{F}_{\alpha\beta}^*/kT(x)$ curves corresponding to ϵ between 0.4 and 0.8 are similar, whereas the $\epsilon = 0.2$ curve exhibits a noticeably lower minimum. As will become evident from later discussion, predictions in which $\epsilon \le 0.2$ tend to differ from those evaluated at larger ϵ.

Recently reported[22] small-angle X-ray scattering (SAXS) data indicate that ordered block copolymer binary blends exhibiting lamellae are immiscible when $N_\alpha/N_\beta > 5$ or, conversely, $\epsilon < 0.2$. The existence of an immiscibility window should be manifested in the change in free energy upon mixing ($\Delta\mathcal{F}^*$), which is determined from $\mathcal{F}_{\alpha\beta}^* - x\mathcal{F}_\alpha^* - (1 - x)\mathcal{F}_\beta^*$. Recalling that $N_\beta = \epsilon N_\alpha$, $\Delta\mathcal{F}^*/kT$ can be conveniently written as

$$\frac{\Delta\mathcal{F}^*}{kT} = \frac{\mathcal{F}_\alpha^*}{kT}[\Psi^{1/3} - x - (1 - x)\epsilon^{-2/3}] + \frac{2\Sigma(x)}{\mu N_\alpha} \tag{27}$$

Predictions from eq 27 are presented as a function of x in Figure 5 and show that $\Delta\mathcal{F}^*$ is negative over $0 < x < 1$ for $0.2 < \epsilon < 0.8$. As seen in Figure 4, each $\Delta\mathcal{F}^*/kT(x)$ curve exhibits a minimum, which is located at $x \approx 0.4$ when $\epsilon > 0.5$, and positive curvature between $x = 0$ and $x = 1$. Positive curvature, a prerequisite for phase miscibility, is retained even when ϵ is as low as 0.01, suggesting that lamellar diblock copolymer blends are infinitely miscible. This predicted behavior is, however, contrary to experimental observations.

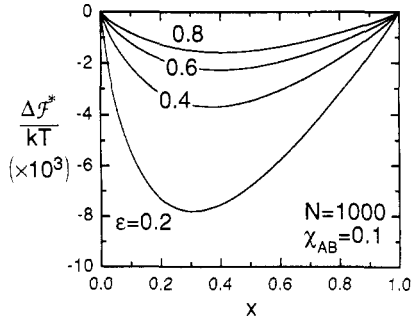

Figure 5. Predicted free energy of mixing, $\Delta\mathcal{F}^*(x)$, for the same values of ϵ shown in Figure 4. In all cases, the curves lie below $\Delta\mathcal{F}^* = 0$ and exhibit positive curvature. Since negative curvature is prerequisite for phase separation, the characteristics of the curves displayed here are indicative of complete blend miscibility. As the α and β blocks become comparable in length (i.e., $\epsilon \to 1$), $\Delta\mathcal{F}^*(x) \to 0$.

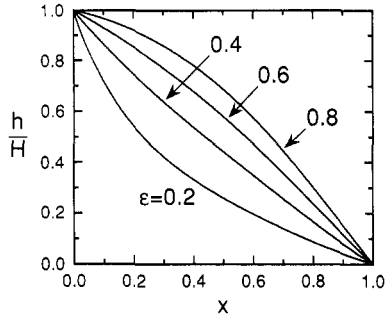

Figure 6. Relative size of the $\alpha + \beta$ mixed layer (h/H) presented as a function of x for four values of ϵ: 0.2, 0.4, 0.6, and 0.8. For small ϵ, $h/H(x)$ decreases rapidly with x, reflecting the disparity in block lengths. As ϵ is increased and the length of the α and β blocks become comparable, $h/H(x)$ changes curvature from positive to negative (at $\epsilon \approx 0.5$) and decreases less dramatically with x.

Phase separation in blends of lamellar diblock copolymers may be the result of thermodynamic equilibrium, in which case simplifying assumptions made here, such as the one regarding random block mixing, appear to render the free energy function incapable of predicting phase immiscibility, as signified by negative curvature in $\Delta\mathcal{F}^*/kT(x)$, and must therefore be refined for small ϵ. Another possibility is that phase separation may result when two populations of copolymer molecules of significantly disparate chain lengths undergo sequential microphase ordering and self-assemble independently during processing (e.g., solvent removal). Since it is presently unclear which of these mechanisms is responsible for observed copolymer immiscibility, further work is needed to identify more precisely the conditions favoring copolymer/copolymer phase separation, especially in binary blends of copolymers possessing dissimilar morphologies.[25]

The dependence of the mixed layer (h) on x for various ϵ is displayed relative to the lamellar half-thickness (H) in Figure 6. These $h/H(x)$ curves apply to both A and B microdomains, since the relative sizes of these layers in A and B lamellae are proportional (through molecular composition). At $x = 0$, the alternating lamellae consist of only β blocks, in which case $h = H$ according to Figure 2. As x is increased, h/H for small ϵ is seen to decrease abruptly as the fraction of α blocks increases. This trend is in conceptual agreement with the illustration presented in Figure 1. Note that the predicted decrease in h/H is nonlinear in x when $\epsilon = 0.2$. As ϵ is increased, however, the curvature of $h/H(x)$ changes from positive to negative so that, at $\epsilon \approx 0.5$, h/H can be accurately represented by $1 - x$. When $\epsilon > 0.5$, the mixed layer still decreases with x but remains a significant fraction of H, reflecting the comparable sizes of the indigenous α and β blocks. As $\epsilon \to 1$ and $N_\beta \to N_\alpha$, $h/H \to 1$ for all x, in agreement with intuitive expectation.

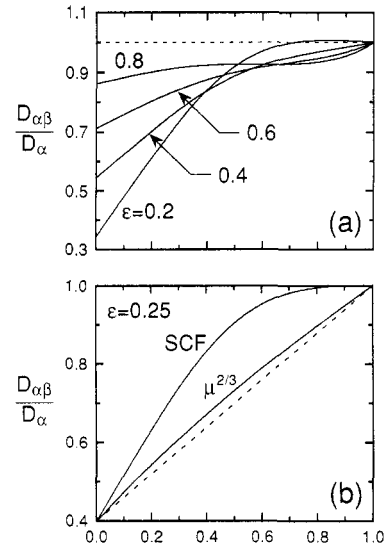

Figure 7. Functional characteristics of $D_{\alpha\beta}/D_\alpha(x)$ obtained by minimizing $\mathcal{F}$. In (a), $D_{\alpha\beta}/D_\alpha$ curves are presented for the same four ϵ employed in previous figures and reveal that blend periodicities do not obey a simple mixing rule. Note that a maximum beyond unity is predicted when ϵ is relatively small and the α and β copolymers possess substantially different chain lengths. A comparison of $D_{\alpha\beta}/D_\alpha$ obtained for $\epsilon = 0.25$ from the present SCF formalism and from the empirical $\mu^{2/3}$ approximation proposed by Hashimoto et al.[22] is provided in (b). Both curves deviate positively from a linear weighting of the neat copolymer periodicities (dashed line).

Figure 7 shows the effect of mixing two infinitely miscible copolymers on the microdomain period ($D_{\alpha\beta}$) relative to that of the pure α copolymer (D_α), as determined from eq 23. In Figure 7a, predicted $D_{\alpha\beta}/D_\alpha$ are provided as a function of x for the same ϵ employed in Figure 6. At $x = 0$, $D_{\alpha\beta} = D_\beta = D_\alpha\epsilon^{-2/3}$. As ϵ is increased, the relative magnitude of D_β increases until $D_\beta = D_\alpha$ and $D_{\alpha\beta}/D_\alpha = 1$ at $\epsilon = 1$. The increase in $D_{\alpha\beta}/D_\alpha$ accompanying x is seen to be highly nonlinear for all ϵ shown in Figure 7a. When $\epsilon < 0.6$, the $D_{\alpha\beta}$ curves exhibit negative curvature over $0 < x < 1$. An interesting feature in this figure is that the curve corresponding to $\epsilon = 0.2$ exceeds $D_{\alpha\beta}/D_\alpha = 1$ (by 0.7%) when x lies between 0.8 and 1.0. It is curious that this feature coincides with (i) anomalous predictions for $\mathcal{F}_{\alpha\beta}^*/kT$ (see Figure 4) and (ii) the onset of apparent[22] α/β immiscibility. While similar, but more pronounced, behavior is observed at smaller ϵ, curves with $\epsilon \geq 0.6$ possess negative curvature at low x and positive curvature at high x. In fact, predicted $D_{\alpha\beta}/D_\alpha$ appear virtually independent of x from $x = 0.5$ to $x = 0.7$ when $\epsilon = 0.8$. Thus, Figure 7a clearly demonstrates that $D_{\alpha\beta}/D_\alpha(x)$ does not obey a simple mixing rule.

Hashimoto et al.[22] have suggested that $D_{\alpha\beta}$ can be discerned from theoretical descriptions of neat diblock copolymers if $\bar{M}_{n,\alpha\beta}$ is calculated as $x\bar{M}_{n,\alpha} + (1 - x)\bar{M}_{n,\beta}$, where $\bar{M}_{n,i}$ denotes the number-average molecular weight of i (i = α, β, or $\alpha\beta$). In terms of the present framework, this expression for monomolecular copolymers is readily translated into $D_{\alpha\beta}/D_\alpha = \mu^{2/3}$, where μ was previously defined as $x + \epsilon(1 - x)$. Curves obtained from the SCF theory presented here and from the empirical approximation of Hashimoto et al.[22] are compared in Figure 7b for $\epsilon = 0.25$. While both $D_{\alpha\beta}/D_\alpha(x)$ curves deviate positively from a linear weighting of D_α and D_β, the one predicted

Table 1. Characteristics of the SI Diblock Copolymer Blends[22] to Which Predictions Are Compared

miscibility	α/β	designation	$\bar{M}_n \times 10^{-3}$	w_S[a]	N[b]	morphology	ϵ[c]	ϵ[d]
full	α	HS-10	81.4	0.63	955	lamellar		
	β	HK-7	31.9	0.35	386	lamellar	0.392	0.404
full	α	HY-10	164	0.69	1911	OBDD		
	β	HY-8	31.6	0.48	377	lamellar	0.193	0.197
partial	α	HS-10	81.4	0.63	955	lamellar		
	β	HK-17	8.5	0.50	101	disordered	0.104	0.106
partial	α	HY-12	534	0.49	6367	lamellar		
	β	HY-8	31.6	0.48	377	lamellar	0.059	0.059

[a] Denotes S weight fraction. [b] Based on $\rho_S = 10100$ mol/m^3, $\rho_I = 13800$ mol/m^3, $b_S = 0.68$ nm, and $b_I = 0.59$ nm. [c] Calculated from $\bar{M}_{n,\beta}/\bar{M}_{n,\alpha}$. [d] Calculated from N_β/N_α.

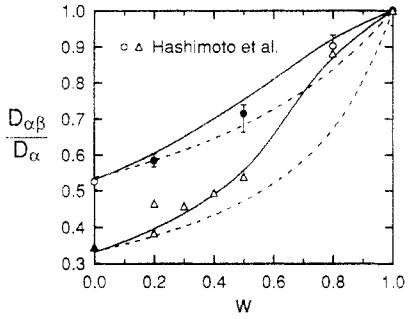

Figure 8. Predicted microdomain periodicities compared with SAXS data[22] for two miscible $(SI)_\alpha/(SI)_\beta$ diblock copolymer blends: (○) HK-7/HS-10 and (△) HY-8/HY-10 (see Table 1 for copolymer and blend characteristics). As seen in Figure 7, the shape of each $D_{\alpha\beta}/D_\alpha(x)$ curve is dictated by ϵ. Agreement between SCF predictions (solid lines) and data appears favorable over the entire composition range, even though some of the HK-7/HS-10 blend morphologies are nonlamellar (●) and the neat HY-10 copolymer exhibits the OBDD morphology (▲). Predicted $D_{\alpha\beta}/D_\alpha$ from the $\mu^{2/3}$ approximation[22] (dashed lines) are observed to underestimate the data.

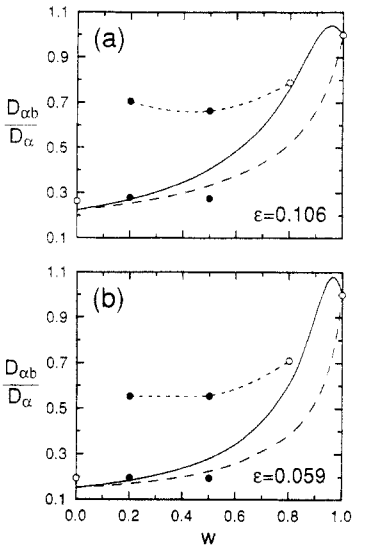

Figure 9. Comparison of predicted $D_{\alpha\beta}/D_\alpha$ with SAXS data[22] for two partially immiscible $(SI)_\alpha/(SI)_\beta$ blends, the characteristics of which are listed in Table 1. Data from the HK-17/HS-10 (a) and HY-8/HY-12 (b) blends are displayed as (○) when one phase exists. Self-consistent field predictions for $D_{\alpha\beta}/D_\alpha$ (solid lines) agree well with single-phase data, while those from the $\mu^{2/3}$ approximation[22] (large dashed lines) underestimate the data. Data from the two-phase regime are shown as (●) and, for the α phase, are connected by short dashed lines as guides for the eye. Since the immiscible α phase in either blend series is not pure, its composition can be estimated from $D_{\alpha\beta}/D_\alpha$.

from the SCF theory is significantly more nonlinear, attaining unity at $x \approx 0.9$.

In this section, predicted $D_{\alpha\beta}/D_\alpha$ are compared with SAXS data[22] for two miscible $(SI)_\alpha/(SI)_\beta$ blends to ascertain the accuracy of the present theoretical approach. Designations and molecular characteristics of the constituent copolymers, including molecular weight ($\bar{M}_n$) and composition, are provided in Table 1. While ϵ for each blend can be estimated from $\bar{M}_{n,\beta}/\bar{M}_{n,\alpha}$ if the copolymer compositions are comparable, values of ϵ should be generally determined from N_β/N_α, in which case $\bar{M}_{n,\alpha}$ and $\bar{M}_{n,\beta}$ must be recast in terms of N_α and N_β, respectively, by following the protocol proposed by Owens et al.[36] The monomer number for each copolymer is determined from $\sum_{i=S,I} N_i(b_i/b_i')^2$, where $b_i' = b_i(\rho_i/\rho')^{1/2}$ and $\rho' = (\rho_S\rho_I)^{1/2}$. Monomer densities ($\rho_i$) and lengths ($b_i$) for S and I are provided in Table 1. Also included in Table 1 are density-corrected values of N, along with the corresponding ϵ for each blend. Note that these ϵ do not differ by more than 3% from those obtained above. To further facilitate comparison between predictions and data, the mole fractions (x) used up to now to represent blend compositions must be converted to weight fractions (w). This is easily accomplished by recognizing that $w = x/\mu$.

Predictions and data for two series of miscible $(SI)_\alpha/(SI)_\beta$ blends are subsequently presented as $D_{\alpha\beta}/D_\alpha(w)$ in Figure 8. As is apparent from this figure, predicted $D_{\alpha\beta}/D_\alpha$ are in remarkably good agreement with the data over the entire composition range. In contrast, $D_{\alpha\beta}/D_\alpha$ obtained from the $\bar{M}_{n,\alpha\beta}$ approximation[22] tend to underestimate the data. It is of interest to note that in the HK-7/HS-10 blend, wherein the α copolymer is HS-10 (see Table 1), some of the blends do *not* exhibit the lamellar morphology. Instead, the morphology observed at $w = 0.2$ remains presently unidentified, while the one at $w = 0.5$ appears cylindrical or ribbon-like. Similar nonlamellar morphologies have been previously observed[25] in binary blends consisting of lamellar and nonlamellar copolymers. Even though these intermediate morphologies are nonlamellar, predicted D from the present formalism for lamellar copolymer blends are seen in Figure 8 to agree reasonably well with the data. Quantitative agreement is also apparent for the neat HY-10 copolymer, which exhibits the OBDD morphology. It must be borne in mind, however, that the present theoretical framework has been derived for the lamellar morphology and, without appropriate modifications to account for interfacial curvature, should not be employed to predict the characteristics of nonlamellar morphologies.

Detailed microstructural characteristics of three series of blends exhibiting partial miscibility have also been recently reported.[22] Only two of those series are displayed in Figure 9, since one series consisted of a copolymer possessing $\bar{M}_n > 10^6$. [Due to its high molecular weight, the neat copolymer, as well as blends with another copolymer, may be incapable of achieving equilibrium.] The relationship $D_{\alpha\beta}/D_\alpha(w)$ for each of the two blends in Figure 9 appears qualitatively similar: (a) the periodicity of the neat β copolymer at $x = 0$ is well-approximated by $\epsilon^{-2/3}$, even if one constituent copolymer (HK-17) is disordered; (b) an immiscibility gap (signified by two

distinct periodicities) exists between $w \approx 0.2$ and $w \approx 0.7$; and (c) single-phase behavior with one characteristic periodicity is recovered when $w \geq 0.8$. Since $x = w\mu$ and $\mu = x + \epsilon(1 - x)$, the observed immiscibility regimes correspond to $0.03 < x < 0.2$ (HK-17/HS-10 with $\epsilon = 0.106$) and $0.02 < x < 0.1$ (HY-8/HY-12 with $\epsilon = 0.059$). The fraction of α copolymer molecules responsible for immiscibility in each of these two blends is therefore relatively small, less than about 20%. In fact, a very small fraction of α molecules (ca. 2–3%) appear sufficient to induce macrophase separation in these blends.

Predicted $D_{\alpha\beta}/D_\alpha$ from the $\bar{M}_{n,\alpha\beta}$ approximation[22] are seen in Figure 9 to underestimate the single-phase data between $w = 0$ and $w = 1$, whereas those obtained from the SCF formalism are again in favorable agreement with the data. In accord with Figure 7a, the SCF predictions exceed unity by 4% in Figure 9a and 8% in Figure 9b when $w > 0.91$ in both of the blend series displayed (HK-17/HS-10 and HY-8/HY-12, respectively). While no attempt is made here to explain this behavior, it should be remembered that experimental data are presently unavailable over the range $0.9 \leq w \leq 1.0$ to discern whether this feature represents a genuine blend characteristic or a mathematical anomaly.

As noted earlier, the present formalism is incapable of predicting partial immiscibility or coexisting microstructures resulting from phase separation. The data from Hashimoto et al.[22] do, however, reveal an important characteristic regarding copolymer partitioning in the two-phase regime: the α phase is *not* pure α, as evidenced in Figure 9 by the substantial decrease in $D_{\alpha\beta}/D_\alpha$ from unity, while the β phase remains almost pure β. The latter feature suggests that the significantly longer α molecules are almost completely excluded from β lamellae, which would be consistent with post-α microphase separation of the β copolymer. Inclusion of β molecules in α-rich lamellae, on the other hand, is expected should the α molecules order prior to the β molecules. Since the α-rich phase constitutes a miscible blend of α and β, its composition (denoted by a prime) can be estimated from the experimental microdomain periodicity. Values of $D_{\alpha\beta}/D_\alpha$ for the α-rich lamellae in Figure 9 are taken as 0.68 (Figure 9a) and 0.55 (Figure 9b), in which case the corresponding α-phase compositions are $w' \approx 0.76$ ($x' \approx 0.25$) and $w' \approx 0.77$ ($x' \approx 0.16$), respectively. Thus, while the present formalism is incapable of predicting copolymer immiscibility from ϵ and x, it is capable of elucidating the compositions of the discrete phases in immiscible blends.

Addendum

Mayes et al.[37] have recently used neutron reflectivity to examine the existence of intramicrodomain localization of long and short blocks in ordered poly(styrene-*b*-methyl methacrylate) diblock copolymer blends possessing the lamellar morphology. Their results reveal that short blocks preferentially reside in close proximity to interphase regions and that D scales as $\bar{M}_n^{2/3}$ for ϵ between 0.25 and 0.40.

Conclusions

A self-consistent field theory employing principles originally developed for neat diblock[31] and triblock[32] copolymers is proposed for miscible binary blends composed of strongly segregated AB diblock copolymers. It has been demonstrated that the free energy and microdomain periodicity of a blend can be conveniently referenced with respect to one of the blend constituents. While partial immiscibility has been observed[22] over a relatively narrow mole fraction range in $(SI)_\alpha/(SI)_\beta$ blends with $N_\beta/N_\alpha \leq 0.1$, free energy predictions obtained here suggest that blends of chemically identical diblock copolymers should be infinitely miscible despite chain length disparity. Whether observed immiscibility reflects thermodynamic equilibrium or a kinetic limitation (e.g., sequential microphase ordering) has yet to be conclusively determined. Predicted microstructural dimensions are found to be in excellent agreement with experimental data[22] and reveal that intramicrodomain mixing of α and β blocks is not ideal, due to differences in chain packing under the constraint of constant density.

Acknowledgment. Sincere gratitude is extended to Air Products and Chemicals, Inc., for support, Mr. J. H. Laurer for assistance in figure production, and Dr. T. P. Russell (IBM) for a preprint of ref. 37.

Appendix

Minimization of the free energy functions F_h' and F_Δ' in eqs 4 and 13, respectively, subject to the constraints placed upon mass and constant density is accomplished through the use of Lagrange multipliers. Following Zhulina and Halperin,[32] the functions Ω_h and Ω_Δ are introduced such that

$$\Omega_h = \frac{F_h'}{kT} - \int_0^h \tilde{\lambda}(\eta)\, d\eta \int_0^\eta E_\beta^{-1}(r,\eta)\, dr - \tilde{\omega} \int_0^h E_\alpha^{-1}(r)\, dr - B \int_0^h \tilde{\psi}(r)\, dr \left[x E_\alpha^{-1}(r) + (1-x)\int_r^h g(\eta) E_\beta^{-1}(r,\eta)\, d\eta\right] \quad \text{(A.1a)}$$

and

$$\Omega_\Delta = \frac{F_\Delta'}{kT} - \int_h^H \tilde{\kappa}(\delta)\, d\delta \int_h^\delta E_\alpha^{-1}(r,\delta)\, dr - Bx \int_h^H \tilde{\gamma}(r)\, dr \left[\int_r^H g(\delta) E_\alpha^{-1}(r,\delta)\, d\delta\right] \quad \text{(A.1b)}$$

where $B = b^3/\sigma$. Substitution of F_h' into eq A.1a and F_Δ' into eq A.1b, followed by algebraic rearrangement and incorporation of numerical coefficients into the Lagrange multipliers (thereby eliminating the ˜), yields

$$\Omega_h = A\left[x\int_0^h I(r)\, dr + (1-x)\int_0^h d\eta \int_0^\eta J(r,\eta)\, dr\right] \quad \text{(A.2a)}$$

$$\Omega_\Delta = Ax \int_h^H d\delta \int_h^\delta K(r,\delta)\, dr \quad \text{(A.2b)}$$

where $A = 3/2b^2$,

$$I(r) = E_\alpha(r) - \omega E_\alpha^{-1}(r) - \psi(r) E_\alpha^{-1}(r) \quad \text{(A.3a)}$$

$$J(r,\eta) = g(\eta) E_\beta(r,\eta) - \lambda(\eta) E_\beta^{-1}(r,\eta) - \psi(r) g(\eta) E_\beta^{-1}(r,\eta) \quad \text{(A.3b)}$$

for the mixed $\alpha + \beta$ (h) layer and

$$K(r,\delta) = g(\delta) E_\alpha(r,\delta) - \kappa(\delta) E_\alpha^{-1}(r,\delta) - \gamma(r) g(\delta) E_\alpha^{-1}(r,\delta) \quad \text{(A.4)}$$

for the Δ layer. Upon differentiating eqs A.3 and A.4 with respect to E_β and E_α and recognizing that $E_\beta(\eta,\eta) = E_\alpha(\delta,\delta) = 0$, the functional forms of $E_\beta(r,\eta)$, $E_\alpha(r)$, and $E_\alpha(r,\delta)$ are discerned as

$$E_\beta(r,\eta) = [\psi(\eta) - \psi(r)]^{1/2} \quad \text{(A.5a)}$$

$$E_\alpha(r) = [\omega - \psi(r)]^{1/2} \tag{A.5b}$$

$$E_\alpha(r,\delta) = [\gamma(\delta) - \gamma(r)]^{1/2} \tag{A.5c}$$

Equations A.5a and A.5c are substituted into eqs 5a and 14, respectively, which can be rearranged to yield Abel integral equations of the form[38]

$$f(r) = \int_a^r \frac{\Theta(s)\,ds}{(r-s)^{1/2}} \tag{A.6}$$

If f' is used here to denote df/dr, the functionality of $\Theta(r)$ is given by

$$\Theta(r) = \frac{1}{\pi}\left[\frac{f(a)}{(r-a)^{1/2}} + \int_a^r \frac{f'(s)\,ds}{(r-s)^{1/2}}\right] \tag{A.6a}$$

from which follow

$$\psi(r) = (\pi r/2\epsilon N_\alpha)^2 \tag{A.7a}$$

$$\gamma(r) = [\pi r/2(1-\Gamma)N_\alpha]^2 + h \tag{A.7b}$$

and, upon subsequent substitution into eqs A.5a and A.5c above, eqs 7a and 16 in the text. Casting $E_\alpha(r)$ (eq A.5b) into the same form as $E_\beta(r,\eta)$ or $E_\alpha(r,\delta)$ introduces Λ (eq 7b), which is found to equal $h\csc(\pi\Gamma/2\epsilon)$ from eq 5b.

With each of the local elastic free energy terms identified, the free energy functions describing the h and Δ layers can be expressed as

$$\frac{F_h'}{kT} = \frac{\pi A}{2\epsilon N_\alpha}\int_0^h f_h(r)\,dr \tag{A.8a}$$

$$\frac{F_\Delta'}{kT} = \frac{\pi A}{2(1-\Gamma)N_\alpha}\int_h^H f_\Delta(r)\,dr \tag{A.8b}$$

where

$$f_h(r) = x(\Lambda^2 - r^2)^{1/2} + (1-x)\int_r^h g(\eta)(\eta^2 - r^2)^{1/2}\,d\eta \tag{A.9a}$$

$$f_\Delta(r) = x\int_r^H g(\delta)(\delta^2 - r^2)^{1/2}\,d\delta \tag{A.9b}$$

Upon comparing eqs A.9a and A.9b with eqs 6 and 15, respectively, it is apparent that $df_h(r)/dr = -\pi r(2\epsilon N_\alpha B)^{-1}\Phi_h(r)$ and $df_\Delta(r)/dr = -\pi r[2(1-\Gamma)N_\alpha B]^{-1}\Phi_\Delta(r)$. Since $\Phi_h(r) = \Phi_\Delta(r) = 1$, $f_h(r) = -\int_r^h[df_h(t)/dt]\,dt + f_h(h)$ and $f_\Delta(r) = -\int_r^H[df_\Delta(t)/dt]\,dt + f_\Delta(H)$, eqs A.8a and A.8b may be analytically evaluated to obtain eqs 8 and 17, respectively, in the text.

References and Notes

(1) Jérôme, R.; Fayt, R.; Teyssié, Ph. In *Thermoplastic Elastomers: A Comprehensive Review*; Legge, N. R., Holden, G., Schroeder, H. E., Eds.; Hanser: Munich, 1987.
(2) Samulski, E. T.; DeSimone, J. M.; Hunt, M. O., Jr.; Menceloglu, Y. Z.; Jarnagin, R. C.; York, G. A.; Labat, K. B.; Wang, H. *Chem. Mater.* **1992**, *4*, 1153.
(3) Smith, S. D.; Ashraf, A.; Clarson, S. J. *Polym. Prepr. (Am. Chem. Soc., Div. Polym. Chem.)* **1993**, *34*, 672.
(4) Matyjaszewski, K.; Moore, M. K.; White, M. L. *Macromolecules* **1993**, *26*, 6741.
(5) Kresge, C. T.; Leonowicz, M. E.; Roth, W. J.; Vartuil, J. C.; Beck, J. S. *Nature* **1992**, *359*, 710.
(6) Burdon, J. W.; Calvert, P. *Mater. Res. Soc. Symp. Proc.* **1991**, *218*, 203.
(7) Thomas, E. L.; Alward, D. B.; Kinning, D. J.; Martin, D. C.; Handlin, D. L.; Fetters, L. J. *Macromolecules* **1986**, *19*, 2197. Hasegawa, H.; Tanaka, H.; Yamasaki, K.; Hashimoto, T. *Macromolecules* **1987**, *20*, 1651.
(8) Hajduk, D. A.; Harper, P. E.; Gruner, S. M.; Honeker, C. C.; Kim, G.; Thomas, E. L.; Fetters, L. J. *Macromolecules* **1994**, *27*, 4063.
(9) Winey, K. I.; Thomas, E. L.; Fetters, L. J. *J. Chem. Phys.* **1991**, *95*, 9367. Winey, K. I.; Thomas, E. L.; Fetters, L. J. *Macromolecules* **1992**, *25*, 422, 2645.
(10) Spontak, R. J.; Smith, S. D.; Ashraf, A. *Macromolecules* **1993**, *26*, 956.
(11) Hashimoto, T.; Tanaka, H.; Hasegawa, H. *Macromolecules* **1990**, *23*, 4378. Tanaka, H.; Hasegawa, H.; Hashimoto, T. *Macromolecules* **1991**, *24*, 240. Tanaka, H.; Hashimoto, T. *Macromolecules* **1991**, *24*, 5712.
(12) Winey, K. I.; Thomas, E. L.; Fetters, L. J. *Macromolecules* **1991**, *24*, 6182.
(13) Matsushita, Y.; Torikai, N.; Mogi, Y.; Noda, I.; Han, C. C. *Macromolecules* **1993**, *26*, 6346.
(14) Hashimoto, T.; Tanaka, H.; Iizuka, N. In *Space-Time Organization in Macromolecular Fluids*; Tanaka, F., Doi, M., Ohta, T., Eds.; Springer-Verlag: Berlin, 1989.
(15) Shull, K. R.; Winey, K. I. *Macromolecules* **1992**, *25*, 2637.
(16) Banaszak, M.; Whitmore, M. D. *Macromolecules* **1992**, *25*, 2757.
(17) Tucker, P. S.; Barlow, J. W.; Paul, D. R. *Macromolecules* **1988**, *21*, 1678, 2794.
(18) Hashimoto, T.; Kimishima, K.; Hasegawa, H. *Macromolecules* **1991**, *24*, 5704.
(19) Xie, R.; Yang, B.; Jiang, B. *Macromolecules* **1993**, *26*, 7097.
(20) Dalvi, M. C.; Lodge, T. P. *Macromolecules* **1993**, *26*, 859.
(21) Hashimoto, T. *Macromolecules* **1982**, *15*, 1548.
(22) Hashimoto, T.; Yamasaki, K.; Koizumi, S.; Hasegawa, H. *Macromolecules* **1993**, *26*, 2895.
(23) Hadziioannou, G.; Skoulios, A. *Macromolecules* **1982**, *15*, 267.
(24) Schwark, D. W. Ph.D. Thesis, University of Massachusetts at Amherst, 1991.
(25) Spontak, R. J.; Smith, S. D.; Satkowski, M. M.; Ashraf, A. Presented at the ACS Central Regional Meeting, Cincinnati, OH, 1992; to be submitted to *Macromolecules*.
(26) Leibler, L.; Benoit, H. *Polymer* **1981**, *22*, 195.
(27) Hong, K. M.; Noolandi, J. *Polym. Commun.* **1984**, *25*, 265.
(28) Spontak, R. J.; Williams, M. C. *J. Polym. Sci., Polym. Phys. Ed.* **1990**, *28*, 1379.
(29) Birshtein, T. M.; Liatskaya, Yu. V.; Zhulina, E. B. *Polymer* **1990**, *31*, 2185. Zhulina, E. B.; Birshtein, T. M. *Polymer* **1991**, *32*, 1299. Lai, P.-Y.; Zhulina, E. B. *Macromolecules* **1992**, *25*, 5201.
(30) Dan, N.; Tirrell, M. *Macromolecules* **1993**, *26*, 6467.
(31) Semenov, A. N. *Sov. Phys. JETP (Engl. Transl.)* **1985**, *61*, 731.
(32) Zhulina, E. B.; Halperin, A. *Macromolecules* **1992**, *25*, 5730.
(33) Helfand, E.; Wasserman, Z. R. *Macromolecules* **1976**, *9*, 879. See also: Fredrickson, G. H.; In *Physics of Polymer Surfaces and Interfaces*; Sanchez, I. C., Ed.; Butterworth-Heinemann: Boston, 1992.
(34) Alexander, S. *J. Phys. (Fr.)* **1977**, *38*, 977.
(35) Melenkevitz, J.; Muthukumar, M. *Macromolecules* **1991**, *24*, 4199.
(36) Owens, J. N.; Gancarz, I. S.; Koberstein, J. T.; Russell, T. P. *Macromolecules* **1989**, *22*, 3380.
(37) Mayes, A. M.; Russell, T. P.; Deline, V. R.; Satija, S. K.; Majkrzak, C. F. *Macromolecules*, in press.
(38) Bronshtein, I. N.; Semendydyev, K. A. *Handbook of Mathematics*; Van Nostrand: New York, 1985.